permafrost
cci

CCI+ PHASE 1 – NEW ECVS
PERMAFROST

D2.1 PRODUCT VALIDATION AND ALGORITHM SELECTION REPORT (PVASR)

VERSION 1.0

15 JANUARY 2019

PREPARED BY

b·geos
GAMMA REMOTE SENSING
UiO : University of Oslo
AWI
UNI FR
UNIVERSITÉ DE FRIBOURG
UNIVERSITÄT FREIBURG
Stockholm University
West University of Timisoara
TERRASIGNA

Document Status Sheet

Issue	Date	Details	Authors
0.1	04.12.2018	Initial version	TS
0.2	17.12.2018	Structure update	AB, SW
0.3	11.01.2019	Draft version	SW, AB, TS
0.4	13.01.2019	First revision	AB
1.0	15.01.2019	Final version	AB, SW

Author team

Annett Bartsch, B.GEOS

Sebastian Westermann, GUIO

Tazio Strozzi, GAMMA

ESA Technical Officer:

Frank Martin Seifert

EUROPEAN SPACE AGENCY CONTRACT REPORT

The work described in this report was done under ESA contract. Responsibility for the contents resides in the authors or organizations that prepared it.

TABLE OF CONTENTS

EXECUTIVE SUMMARY

The Product Validation and Algorithm Selection Report (PVASR) describes the analysis done in the round robin inter-comparison, the results achieved, and the algorithm selections made.

The parameters to be retrieved comprise ground temperature and active layer thickness. Ground temperature forms also the basis for permafrost fraction as also requested by user groups. Results of the round robin are discussed with respect to the user requirements, including geographical coverage, temporal sampling, temporal extent, horizontal resolution, subgrid variability, vertical resolution, vertical extent, precision and accuracy.

In a first step, algorithms have been reviewed with respect to the basic requirements regarding ability to provide all needed parameters, global coverage and temporal and spatial sampling. Suitable approaches are then further assessed with respect to the ability to provide subgrid variability and accuracy based on in situ data.

Ground temperature from borehole data available through GTN-P and active layer thickness through CALM are widely used as validation for permafrost studies and thus form the basis for the benchmarking in Permafrost_cci. The skill of the algorithms is assessed through measures such as correlation, root mean square error and standard deviation.

The round robin contained the following parts: (1) a comparison of the transient permafrost model compile for Permafrost_cci (CryoGrid CCI model) against an independent state-of-the-art permafrost model (GIPL2, UAF Alaska, USA), using the same input data; (2) an evaluation of ground temperature performance against in-situ data taken at borehole sites, as well as a performance comparison with other published studies, and (3) an extended evaluation of CryoGrid CCI performance regarding active layer thickness and permafrost extent/fraction.

Comparison of the CryoGrid CCI and the GIPL2 model shows that the CryoGrid CCI produces highly similar results as GIPL2 over the entire relevant temperature range, showing that the model employed in the Permafrost_cci algorithm can match the performance of the state-of-the-art model framework. Comparison of results of CryoGrid CCI driven by EO-based forcing data with in-situ measurements in boreholes shows a Root Mean Square Error (RMSE) of about 1.9K with respect to permafrost temperature, which is on par or slightly better than most other published studies. For the active layer thickness, a good match is achieved if the ground stratigraphy employed in the modelling is an adequate representation of the true conditions at field sites, highlighting the importance of the permafrost ground stratigraphy product under work in Permafrost_cci. Permafrost fractions have been compared to the results of a deterministic high-resolution (10 m) permafrost model for a highly structured area in the European Alps, which shows that the Permafrost_cci algorithm can represent the gradual decrease of permafrost fractions from the permafrost-dominated high-elevation areas to the permafrost-free valleys.

Finally, the results are discussed with respect of user requirements, showing that the Permafrost_cci algorithm can likely deliver threshold requirements in almost all categories, while likely achieving target requirements for important categories, such as the spatial resolution of the resulting products.

1 INTRODUCTION

1.1 Purpose of the document

This document evaluates the selection of a suitable algorithm in the Permafrost_cci. At present-day, there is no consistent and frequently updated global map of the parameters permafrost temperature and active layer thickness, as required by GCOS [AD-4] based on Earth Observation records, so that permafrost change detection is only possible at localized sites with in-situ observations. The CCI+ Permafrost service will for the first time provide such information for different epochs [AD-1], attempting to meet User requirements (as outline in the URD [RD-1]) as good as possible.

In this document, we discuss the suitability of different published EO-based algorithms for temporally and spatially consistent, global ECV generation. We report on the results of intercomparisons with other permafrost algorithms and model approaches, and provide an assessment of the performance of the first version of the Permafrost_cci algorithm against in-situ data.

1.2 Structure of the document

In Section 2, the context of evaluating the permafrost ECV from space is evaluated, in particular the relation with ground-based in-situ monitoring. Section 3 contains an overview over published EO-based algorithms, comparing their suitability in the light of general CCI requirements and particular requirements for the permafrost ECV. Section 4 displays the results of comparison with other algorithms and in-situ benchmark data sets, outlining priorities for improvements in years 2 and 3. Finally, Section 5 draws the conclusions for algorithm selection in CCI+ Permafrost.

1.3 Applicable Documents

[AD-1] ESA 2017: Climate Change Initiative Extension (CCI+) Phase 1 – New Essential Climate Variables - Statement of Work. ESA-CCI-PRGM-EOPS-SW-17-0032

[AD-2] Requirements for monitoring of permafrost in polar regions - A community white paper in response to the WMO Polar Space Task Group (PSTG), Version 4, 2014-10-09. Austrian Polar Research Institute, Vienna, Austria, 20 pp

[AD-3] ECV 9 Permafrost: assessment report on available methodological standards and guides, 1 Nov 2009, GTOS-62

[AD-4] GCOS-200, the Global Observing System for Climate: Implementation Needs (2016 GCOS Implementation Plan, 2015.

1.4 Reference Documents

[RD-1] Bartsch, A., Matthes, H., Westermann, S., Heim, B., Pellet, C., Onacu, A., Kroisleitner, C., Strozzi, T.(2019): ESA CCI+ Permafrost User Requirements Document, v1.0

[RD-2] Bartsch, A., Westermann, Strozzi, T., Wiesmann, A., Kroisleitner, C. (2019): ESA CCI+ Permafrost Product Specifications Document, v1.0

[RD-3] Bartsch, A., Westermann, S., Heim, B., Wieczorek, M., Pellet, C., Barboux, C., Kroisleitner, C., Strozzi, T. (2019): ESA CCI+ Permafrost Data Access Requirements Document, v1.0

[RD-4] Bartsch, A.; Grosse, G.; Kääb, A.; Westermann, S.; Strozzi, T.; Wiesmann, A.; Duguay, C.; Seifert, F. M.; Obu, J.; Goler, R.: GlobPermafrost – How space-based earth observation supports understanding of permafrost. Proceedings of the ESA Living Planet Symposium, pp. 6.

[RD-5] IPA Action Group 'Specification of a Permafrost Reference Product in Succession of the IPA Map' (2016): Final report.
https://ipa.arcticportal.org/images/stories/AG_reports/IPA_AG_SucessorMap_Final_2016.pdf

[RD-6] GlobPermafrost team (2016): Requirements Baseline Document. ESA DUE GlobPermafrost project. ZAMG, Vienna.

1.5 Bibliography

A complete bibliographic list that support arguments or statements made within the current document is provided in Section 6.1.

1.6 Acronyms

A list of acronyms is provided in section 6.2.

1.7 Glossary

The list below provides a selection of term relevant for the parameters addressed in CCI+ Permafrost. A comprehensive glossary is available as part of the Product Specifications Document [RD-2].

active-layer thickness

The thickness of the layer of the ground that is subject to annual thawing and freezing in areas underlain by permafrost.

The thickness of the active layer depends on such factors as the ambient air temperature, vegetation, drainage, soil or rock type and total water con-tent, snowcover, and degree and orientation of slope. As a rule, the active layer is thin in the High Arctic (it can be less than 15 cm) and becomes thicker farther south (1 m or more).

The thickness of the active layer can vary from year to year, primarily due to variations in the mean annual air temperature, distribution of soil moisture, and snowcover.

The thickness of the active layer includes the uppermost part of the permafrost wherever either the salinity or clay content of the permafrost allows it to thaw and refreeze annually, even though the material remains cryotic (T < 0°C).

Use of the term "depth to permafrost" as a synonym for the thickness of the active layer is misleading, especially in areas where the active layer is separated from the permafrost by a residual thaw layer, that is, by a thawed or noncryotic (T> 0°C) layer of ground.

REFERENCES: Muller, 1943; Williams, 1965; van Everdingen, 1985

continuous permafrost

Permafrost occurring everywhere beneath the exposed land surface throughout a geographic region with the exception of widely scattered sites, such as newly deposited unconsolidated sediments, where the climate has just begun to impose its influence on the thermal regime of the ground, causing the development of continuous permafrost.

For practical purposes, the existence of small taliks within continuous permafrost has to be recognized. The term, therefore, generally refers to areas where more than 90 percent of the ground surface is underlain by permafrost.

REFERENCE: Brown, 1970.

discontinuous permafrost

Permafrost occurring in some areas beneath the exposed land surface throughout a geographic region where other areas are free of permafrost.

Discontinuous permafrost occurs between the continuous permafrost zone and the southern latitudinal limit of permafrost in lowlands. Depending on the scale of mapping, several subzones can often be distinguished, based on the percentage (or fraction) of the land surface underlain by permafrost, as shown in the following table.

Permafrost	English usage	Russian Usage
Extensive	65-90%	Massive Island
Intermediate	35-65%	Island
Sporadic	10-35%	Sporadic
Isolated Patches	0-10%	-

SYNONYMS: (not recommended) insular permafrost; island permafrost; scattered permafrost.

REFERENCES: Brown, 1970; Kudryavtsev, 1978; Heginbottom, 1984; Heginbottom and Radburn, 1992; Brown et al., 1997.

mean annual ground temperature (MAGT)

Mean annual temperature of the ground at a particular depth.

The mean annual temperature of the ground usually increases with depth below the surface. In some northern areas, however, it is not un-common to find that the mean annual ground temperature decreases in the upper 50 to 100 metres below the ground surface as a result of past changes in surface and climate conditions. Below that depth, it will increase as a result of the geothermal heat flux from the interior of the earth. The mean annual ground temperature at the

depth of zero annual amplitude is often used to assess the thermal regime of the ground at various locations.

permafrost

Ground (soil or rock and included ice and organic material) that remains at or below 0°C for at least two consecutive years .

Permafrost is synonymous with perennially cryotic ground: it is defined on the basis of temperature. It is not necessarily frozen, because the freezing point of the included water may be depressed several degrees below 0°C; moisture in the form of water or ice may or may not be present. In other words, whereas all perennially frozen ground is permafrost, not all permafrost is perennially frozen. Permafrost should not be regarded as permanent, because natural or man-made changes in the climate or terrain may cause the temperature of the ground to rise above 0°C. Permafrost includes perennial ground ice, but not glacier ice or icings, or bodies of surface water with temperatures perennially below 0°C; it does include man-made perennially frozen ground around or below chilled pipe-lines, hockey arenas, etc.

Russian usage requires the continuous existence of temperatures below 0°C for at least three years, and also the presence of at least some ice.

SYNONYMS: perennially frozen ground, perennially cryotic ground and (not recommended) biennially frozen ground, climafrost, cryic layer, permanently frozen ground.

REFERENCES: Muller, 1943; van Everdingen, 1976; Kudryavtsev, 1978.

2 CONTEXT OF THE ALGORITHMS AND ACCURACY DETERMINATION

2.1 Context of the algorithms

The required parameters by GCOS for the Permafrost ECV are [AD-1,4]

a) Permafrost temperature (K), and
b) Depth of active layer (m).

At present, terrestrial systems are in place within which these physical variables are monitored at specific sites, either continuously (as typical in boreholes for ground temperature in the GTN-P) or sporadically during a season (as for active layer thickness at CALM sites), or even only every few years. While the terrestrial monitoring has been drastically expanded during and after the "International Polar Year" (IPY), the distribution of sites is strongly biased towards a few regions (typically where resource extraction and/or infrastructure projects have created easy access), leaving vast areas uncovered by monitoring. This in particular renders upcscaling of trends in the permafrost ECV to global scale problematic and complicates validation of Earth System Model output related to permafrost.

The main requirement for EO-based algorithms for permafrost ECV generation is therefore to improve the spatial and, if possible, also the temporal coverage compared to the existing in-situ networks, while at the same time providing consistent coverage of at least all relevant permafrost regions. Since EO-based algorithms necessarily operate at the spatial scale of individual pixels, the spatial resolution of the output must be put in context with the spatial variability of permafrost temperatures and active layer thickness. In many permafrost regions, these can display a strong variability at spatial scales of meters, which is generally much finer than the footprint of EO sensors. For this reason, it makes sense to add an additional variable,

c) Permafrost extent (fraction)

as permafrost ECV parameter, which is the aerial fraction within an area (pixel) at which the definition for the existence of permafrost (ground temperature < 0 ºC for two consecutive years) is fulfilled. The characterization of the permafrost extent in terms of aerial coverage has been employed for decades in the permafrost community, e.g. in the classic IPA permafrost map (Brown et al., 1998) displaying classes of continuous, discontinuous, sporadic and isolated permafrost. Note that permafrost extent could easily be calculated from ground temperature (variable b) if this parameter was accessible at sufficiently fine spatial resolution (i.e. representing the true spatial variability of ground temperatures). If this is not the case, as in real-world applications of EO-based data, permafrost fraction should be added as a parameter, since the average ground temperature within a pixel does not contain information on the spread of temperatures within a pixel: an average ground temperature of +1.5 ºC within a pixel does not necessarily mean that it is free of permafrost, but permafrost can (and is likely to) exist at localized sites, often covering a significant portion of the pixel.

2.2 Accuracy determination

In the ESA GlobPermafrost project, modeling of permafrost extent and temperatures has been performed using a simple model scheme driven by data sets of surface temperature, snow and landcover. Validation has been accomplished with on a collection of in-situ ground temperatures in boreholes, comprising 359 boreholes in the GTN-P (Global Terrestrial Network for Permafrost, Biskaborn et al. 2015), 392 in the TSP (Thermal state of Permafrost) network (International Permafrost Association, 2010), and 169 MAGT measurements from different publications in China (overview in Obu et al., in review). The main advantage of this collection is the relatively favourable spatial coverage, which makes a statistical evaluation possible. Furthermore, it has been employed by other studies (e.g. GlobPermafrost, Obu et al., in review; Wang et al., 2018), so that algorithm performance can be benchmarked for a common data set. On the other side, the collection features the strong disadvantage that neither time of acquisition nor the depth of the temperature measurement are standardized, thus strongly limiting the value of a comparison with algorithm output at a specific depth and time. A comprehensive reprocessing and standardization of in-situ measurements is under way in Permafrost_cci, but not yet operational at this stage.

For active layer thickness, we employ in-situ data by the CALM program downloaded from https://www2.gwu.edu/~calm/data/north.html. At this stage, only exemplary comparisons can be provided, since the ground stratigraphy input for Permafrost_cci is not yet available, which is the critical factor for determination of active layer thickness (see Langer et al., 2013, for a comprehensive sensitivity analysis).

For permafrost fraction, only few in-situ data sets are available, as already pointed out by previous studies (Chadburn et al., 2017). Here, in particular existing maps can serve as benchmark, but also spatially distributed measurements of ground surface or near-surface ground temperatures with arrays of temperature loggers (e.g. Gisnås et al., 2014).

3 ALGORITHMS AVAILABLE FOR PERMAFROST ECV GENERATION BASED ON EO DATA

3.1 Existing algorithms

Remote characterization of the permafrost ECV is a major problem since permafrost does directly not become manifest in a single EO technology. Therefore, some kind of transfer function or model approach must be employed, using either one or several EO products as input, often combined with non-EO-based data sets. In the following, we provide an overview over published methods to characterize the physical variables ground temperature, permafrost extent and active layer thickness with EO data. Table 1 displays a comparison of the different methods. Note that we do not list methods that do not employ EO-data for ECV generation (e.g. Aalto et al., 2018), but we compare their performance compared to the EO-based algorithms in Sect.4.

1. *Identification of surface features characteristic for permafrost*: In some areas, the presence of permafrost in the ground becomes manifest in surface features, in particular landforms related ground ice, such as rock glaciers, pingos, palsas or tundra polygons. These can be detected on high-resolution optical imagery from satellites. Furthermore, ecotypes derived from Landsat classification and terrain data have been shown to be associated to ground temperatures, so that permafrost maps can be compiled in certain areas (Cable et al. 2016). This method requires high thematic detail and is only feasible regionally. Over larger areas, it lacks consistency, as indicators can have different meanings depending on the climate. In Scandinavia, for example, the presence of forest is linked to permafrost-free conditions, while forest in Mongolia and other parts of central Asia is clear evidence of permafrost. In addition, there are no clear surface indicators in many permafrost areas, and a quantitative characterization of the state variables of the permafrost ECV (see Sect. 2.1) is not possible. Therefore, the method is not suited for global ECV characterization in Permafrost_cci, but surface indicators can serve as independent validation for other methods.

2. *Change detection of surface indictors*: Similar to (1), but adding time as an additional component, processes relating to permafrost changes can be made visible. An example is the formation of disappearance of thermokarst lakes (Nitze & Grosse, 2016), that becomes evident in changes of the spectral signature of the surface. In mountain areas, detecting changes in rock glacier velocity is a possibility (e.g. Sorg et al., 2015). In areas with excess ground ice, multi-year surface subsidence can be detected through InSAR For the same reasons as in (1), this class of methods is not suitable for global characterization of the permafrost ECV.

3. *Statistics of the freeze-thaw state and surface temperature determined from microwave sensors*: Surface state statistics have been shown to provide a rough approximation of permafrost extent (Park et al. 2016), as well as the statistics of microwave derived surface temperature which can be translated to ground temperature (Kroisleitner et al., 2018). The Freeze-Thaw to Temperature (FT2T) model has been modified for Permafrost_cci to represent TTOP and thus enable comparability with CryoGrid 2 (Obu et al. in review). Surface state methods have the advantage that they are purely based on satellite data, but show large differences in transition zones depending on the satellite (frequency) and algorithm (freeze/thaw state detection, consideration of melting snow) that has been used. Local conditions (soils and snow) are neglected what further reduces the accuracy. Since daily observation are needed, only scatterometer or passive microwave instruments are suitable, which reduces the spatial detail to a resolution of 12.5 or coarser. Furthermore, in mountain and coastal areas, as well as

areas with a high density of water bodies, the method is expected to perform poorly. The method does not provide active layer thickness.

4. *Active layer thickness (ALT) from remotely sensed landcover*: ALT can be also derived by empirical relationships between probe measurements and landcover attributes measurable by remote sensing. Investigations have been made using the normalized difference vegetation index (NDVI) (e.g. McMichael et al., 1997; Kelley et al., 2004), radar backscatter (Widhalm et al. 2016, 2017), digital elevation data and land cover classes (Nelson et al., 1997; Peddle and Franklin, 1993). A combination with derivatives of digital elevation models (DEMs) has been shown to be of added value (Peddle and Franklin, 1993; Leverington and Duguay, 1996; Gangodagamage et al., 2014). Although the applicability has been demonstrated at local to regional scale, global application is not possible.

5. *Active layer thickness from remotely sensed land surface temperature*: For the estimating of active layer thickness an approach has been proposed which uses an LST derived Annual Thawing Index (ATI) and an Edaphic Factor (EF) that parameterises the effect of land cover type on soil thermal state (Park et al. 2016), using the Stefan equation. This method delivers active layer thickness, but de to prolonged cloudiness, gap filling with data from other sources is necessary. The main problem of the method is its complete insensitivity to the winter conditions at the site. A warm permafrost or even permafrost-free site in a maritime area with warm winters can have the same Annual Thawing Index as a permafrost site with cold winters in a continental climate, but the "active layer thickness" would naturally be very different. At the same time, the method can only detect changes in active layer thickness related to a summer warming, not to winter warming which especially in areas with warm permafrost can lead to active layer deepening. In addition, the Edaphic Factor is a major parameter for active layer determination, which is poorly constrained on the global scale.

6. *Calculation of Active Layer Thickness from InSAR-derived seasonal subsidence/heave signal*: The seasonal subsidence and heave signal of the surface is dependent on the change of the densities of water and ice within the active layer. Under some conditions, this can be used to infer the active layer thickness from time series of InSAR retrievals, especially when the active layer is fully saturated with water (Liu et al, 2012, Schaefer et al, 2015). For unsaturated gravelly soils, the method does not work (Schaefer et al, 2015). Furthermore, coherence is required ideally over the entire thaw season, but at lest between onset of thaw and maximum thaw depth. In many permafrost regions, this is not possible, so that the method does not work.

7. *Equilibrium permafrost modeling driven by LST time series* In the GlobPermafrost project, a simple TTOP equilibrium permafrost model was used to transfer freezing and thawing degree days from remotely sensed LST (from the MODIS sensor), remotely sensed land cover for ESA CCI landcover and snow information to produce a global 1km map of ground temperatures and permafrost fraction (Obu et al., in review). The employed equilibrium model is simple and computationally efficient, but it has two distinct disadvantages in the context of the Permafrost_cci: first, it can only deliver an average ground temperature for periods on the order of a decade, so it is not suitable for change detection. Second, it cannot deliver active layer thickness. However, the general agreement of the resulting map with existing permafrost maps suggests that the employed input data sets are in general suited for permafrost models. Furthermore, the scheme demonstrated that ensemble methods (i.e. modeling many different realizations for a pixel using slightly perturbed input data) can deliver meaningful values for permafrost fraction within 1 km pixels.

8. *Transient permafrost modeling driven by LST time series without ensemble representation*: Recently, Westermann et al., (2017) demonstrated a transient approach based on the CryoGrid 2 model (Westermann et al., 2013) to infer ground temperature and active layer thickness on regional scale for the Lena River Delta in Northeast Siberia, based on similar input data as employed the ESA GlobPermafrost project (method 7). Here, it is crucial to prescribe the spatial variability of ground thermal properties in terms a typical ground stratigraphy. In the presented 1km approach, subgrid variability is not taken into account, so permafrost fractions can only be computed in a binary (yes/no) way. In principle, the method is not limited to employing the CryoGrid 2 model, but other state-of-the-art permafrost models, such as GIPL2 (Jafarov et al., 2012) could be employed in conjunction with EO-base input. However, such has not been demonstrated yet.

9. *Transient permafrost modeling driven by LST time series with ensemble representation*: For CCI+ permafrost, it is planned to combine the method described in (8) with the global input data sets and the ensemble approach established in ESA Glob Permafrost. The compiled algorithm is based on the CryoGrid model (Westermann et al., 2013, 2016), and is in the following denoted "CryoGrid CCI".

*Table 1: Comparison of different methods to quantitatively characterize the permafrost ECV with EO-based data sets on the **global scale**. If in principle possible, the expected performance on global scale is characterized by: - bad, 0 satisfactory, + good. The algorithm proposed for Permafrost_cci is shaded in grey. Note that the assessment only applies to global performance, the methods can produce a much better performance in local studies. See text.*

Method (see above)	**(1)**	**(2)**	**(3)**	**(4)**	**(5)**	**(6)**	**(7)**	**(8)**	**(9)**
Ground temperature	No	No	+	No	No	No	+	+	+
possible time res.			1 yr				10 yr	8d	8d
possible spatial res.			12.5km				1km	1 km	1km
Active Layer Thickness	No	No	No	No	-	No	No	+	+
possible time res.					8d			8d	8d
possible spatial res.					1km			1km	1km
Permafrost fraction	No	No	0	No	No	No	+	-	+
possible time res.			1 yr				10 yr	8d	8d
possible spatial res.			12.5km				1km	1km	1km
Consistent evaluation of ground temperature and active layer thickness	No	No	No	No	No	No	No	+	+

Table 1 shows that method (9) initially proposed for Permafrost_cci is, in principle, best suited to characterize ground temperature, permafrost fraction and active layer thickness. **The spatial and time resolutions that can (in principle) be achieved with the method are enough to satisfy the requirements of most users, as outlined in the URD [RD-1].**

3.2 Conclusions for the round robin

The main purpose of the round robin is to explore that the algorithm implemented for Permafrost_cci is **also in practice** best suited for characterization of the permafrost ECV. Since global application of the algorithm is very time-consuming (runtime >2 months on a supercomputing cluster), it is not run globally, so that the evaluation must be continued in years 2 and 3 of the project. The round robin experiment is structured in three parts:

1) a comparison of the transient permafrost model, based on the CryoGrid CCI model (Westermann et al, 2015) against an independent state-of-the-art permafrost model (GIPL2, UAF Alaska, USA), using the same input data; through this, we can ensure that the performance is not affected by systematic biases in the employed permafrost model.

2) an evaluation of ground temperature performance for borehole sites (see Sect. 2.2), comparing the global performance against methods (3) and (7), as well as other published studies using other sources than EO data to infer ground temperatures.

3) evaluations of active layer thickness and permafrost extent/fraction. Here, only a few sites and regions can be considered at this stage.

4 ANALYSIS AND INTERCOMPARISON OF RESULTS

4.1. Details of model intercomparison of CryoGrid CCI and GIPL2

The GIPL 2 model compiled and maintained by the Geophysical Institute at UAF, Fairbanks, Alaska, USA, is widely considered one of the state-of-the-art transient permafrost models. It is based on the work of the well-known permafrost researchers Vladimir Romanovsky and Sergej Marchenko at UAF. GIPL2 has been for permafrost characterization in a wide variety of setting, also for spatially distributed permafrost mapping (e.g. Jafarov et al., 2012, Daanen et al., 2012). From its structure of input data, it is very similar to CryoGrid CCI, in that it directly accepts time series of surface temperature and snow depth as input.

The purpose of this comparison is to evaluate if the CryoGrid CCI model can match the performance of the published state-of-the-art model GIPL2 with respect to ground thermal modeling (i.e. irrespective of applied forcing data). The comparison was performed with preliminary forcing data and highly preliminary ground stratigraphies, so it is not meaningful to compare the GIPL2 results directly to in-situ borehole temperatures as provided in Table 2 (see next section). We also point out that GIPL2 represents a permafrost model and not a separate method for ECV generation form EO data (as listed in Sect. 3), which would require generation of forcing data from EO products in addition to the permafrost model. However, since the permafrost model is an important part of the Permafrost_cci, it is important to make sure that this part of the processing chain functions properly and does not introduce a bias in the results. Most other state-of-the-art models, such as GeoTop 2.0 (Fiddes et al., 2015), use a surface energy balance formulation instead, so the models cannot be compared for exactly the same input data, making them unsuitable for a direct comparison.

For the round robin experiment, Dr. Dmitry Nicolsky (UAF Alaska, USA, and Moscow State University, Russia) ran GIPL2 with forcing data provided by the CCI+ project, processed from remotely sensed LST, for 920 borehole sites which are distributed over the entire Northern Hemisphere and therefore provide an adequate cross-section of permafrost conditions. The model period was 2003 to 2017, and we use the last 6 years for comparison, since potential differences due to a different spin-up procedure of the two models have vanished by then. Despite similarities, there are some differences in the setup of GIPL2 and CryoGrid CCI, especially concerning the treatment of the snow cover (prescribed snow density in GIPL2 vs. dynamic snow density in CryoGrid CCI) and the parametrization of the soil freezing characteristic. Therefore, a perfect match between model results is not expected, but the setup was chosen as similar as possible to ensure comparability. Fig. 1 shows the results of the model intercomparison, proving that the results of CryoGrid CCI are very similar to GIPL2, with deviations generally less than 1.5 ºC and no systematic bias for any temperature range. The magnitude of the deviations (RMSE 0.25K) is on the order of what can be caused by the above mentioned differences in ground and snow treatment.

Comparison of runtimes between GIPL2 and CryoGrid CCI showed that CryoGrid CCI in its present stage is 2 to 4 times faster than GIPL2. While differences in the employed processors likely exist, this shows that CryoGrid CCI is at least on par with the state-of-the-art model GIPL2 with respect to runtime. Moreover, GIPL2 is implemented in C, i.e. in an efficient compiler language, while CryoGrid

CCI at this stage exists only as Matlab code, which is a significantly slower interpreter language. In year 2 or 3, implementation of CryoGrid CCI in C or the new language julia (https://julialang.org/) is planned, which in general realizes a speed-up of at least factor 5 in runtime, according to previous experiences with implementations of the CryoGrid model. Therefore, it is highly likely that CryoGrid CCI can achieve a significant runtime advantage compared to other state-of-the-art models, while retaining the performance with respect to modeled ground temperatures.

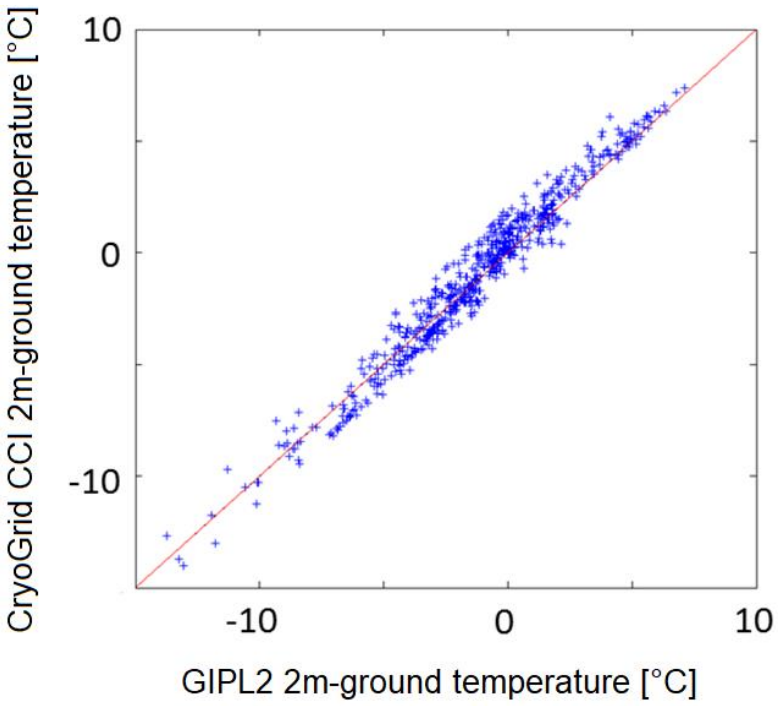

Fig. 1: Modeled 2m- ground temperature (2012-2017, unit ºC) for 920 borehole sites (data set as in Fig. 2) using the GIPL2 model (x-axis) and the CryoGrid CCI (y-axis), with the 1:1 line shown in red. Both models are driven by the same input data of surface temperature and snow (as processed for Permafrost_cci), but feature differences in the representation of ground properties and the snow cover. GIPL2 runs were performed by Dmitry Nicolsky, UAF Fairbanks, USA.

4.2. Performance of different circumpolar to global studies recently published or developed within CCI+ Permafrost

Ground temperature: Fig. 2 shows a comparison of preliminary CryoGrid CCI runs for 920 borehole sites, using the years 2003-2012 for comparison. The depth of 2m was selected since it is well below the active layer for most borehole sites, but at the same time close to the "top of permafrost temperature" (TTOP) inferred in ESA GlobPermafrost. The comparison shows no significant overall bias and a Root Mean Square Error (RMSE) of 1.85 to 1.95 K, depending on the employed ground stratigraphies.

Table 2 provides an overview of reported accuracy from literature and Permafrost_cci initial model improvements. Compared to other recently published studies with global focus, the unoptimized CryoGrid CCI results feature an RMSE with boreholes of similar magnitude, but in general slightly

better (Table 2). The same is true for the 12.5km FT2T CCI algorithm (method 3) which achieves a similar RMSE as CryoGrid CCI. Only the machine learning approach of Aalto et al. (2018) produces a lower RMSE, but it does not represent a physically-based approach that is independent of the borehole data, but rather a best-possible fit to the borehole data. Considering this, it is rather remarkable that the RMSE of CryoGrid CCI and FT2T CCI are still of similar magnitude.

We conclude that the performance of CCI+ Permafrost algorithms with respect to ground temperature is at least similar, probably slightly better than that of other published global model schemes.

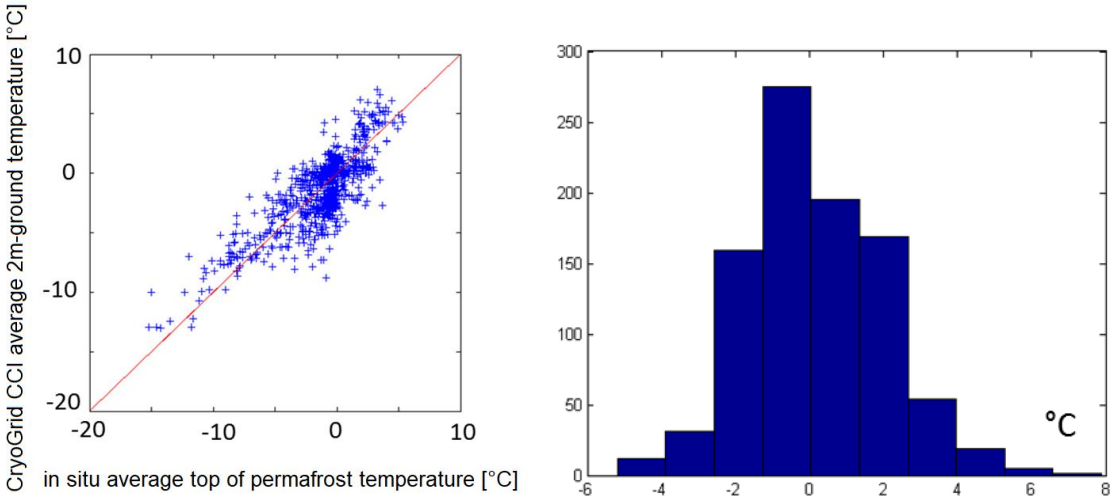

Fig. 2: Left: Measured ground temperature (unit ºC) vs. average modeled ground temperature 2003-2012 (Cryogrid CCI; y-axis, unit ºC) for the 920 boreholes employed for comparison in GGlobPermafrost (CryoGrid2; Obu et al., in review). The RMSE is in this comparison is 1.88K, the bias (measured minus modeled is +0.15K. Right: Histogram of deviations (measured minus modeled, x-axis unit ºC and y-axis number of boreholes), with values ranging between 1.85 and 1.95K (Table 2) depending on the applied ground stratigraphies.

Table 2: Performance of different circumpolar to global studies recently published or developed within Permafrost_cci (FT2T CCI; CryoGrid CCI) for ground temperature in permafrost areas.

Study	Spatial res.	# of boreholes	RMSE	Method (see Table 1)
Obu et al., in review GlobPermafrost	1km	920 TTOP	1.99 K	(7)
Kroisleitner et al., 2018 FT2T	12.5km	216, coldest sensor	2.22 K	(3)
FT2T CCI	12.5km	742 TTOP	1.90 K	(3)
CryoGrid CCI (not yet optimized)	1km	920	1.85-1.95K	(9)
Kang et al., 2018	12.5km	409	2.18 K	GIPL2, no EO data
Aalto et al., 2018	1km	1000	1.6 K	Machine learning, no EO data

Active Layer Thickness: In transient permafrost modeling, as with CryoGrid CCI, the modelled active layer thickness is almost completely controlled by the applied ground stratigraphy (see Langer et al., 2013, for a comprehensive sensitivity analysis). Especially organic (moss) layers at the surface have an enormous impact on modelled active layer thickness, and areas with thick organic layers can feature several times lower active layer thicknesses compared to adjacent areas with mineral ground (e.g. Westermann et al., 2017). Furthermore, ground ice is an important factor for active layer thickness, especially when the active layer deepens in the course of a warming climate. Therefore, a spatially distributed product of ground stratigraphies is required as input to CryoGrid CCI in order to achieve a satisfactory performance for the active layer thickness. At present, such a product does not exist globally, but Permafrost_cci is actively working towards creating an initial version combining various data sources to a global product.

At this point, this new ground stratigraphy product is not yet available, so generic stratigraphies compiled for six landcover classes (tundra, grassland, shrubs, coniferous forest, deciduous forest, wetland) employed in ESA GlobPermafrost (Obu et al., in review) have been employed to compile preliminary benchmarks with respect to active layer thickness. In Figs. 3-7, we present comparisons of modelled active layer thickness for the ensemble (5 members) modelled with CryoGrid CCI. The first two figures (Fig. 3-4, Barrow and Nadym) exemplify cases for which the employed ground stratigraphies are highly adequate for the sites. Fig. 4 (second figure) also shows the effect of the ensemble representation: here, two different ground stratigraphies are present within a pixel, with the coniferous forest stratigraphy (upper two lines) featuring much higher active layer thicknesses compared to tundra (lower three lines), which, on the other hand, correspond very well to measured active layer thicknesses (which are taken at a non-forested site). This clearly exemplifies the significance of an adequate ground stratigraphy product for reproducing active layer thickness.

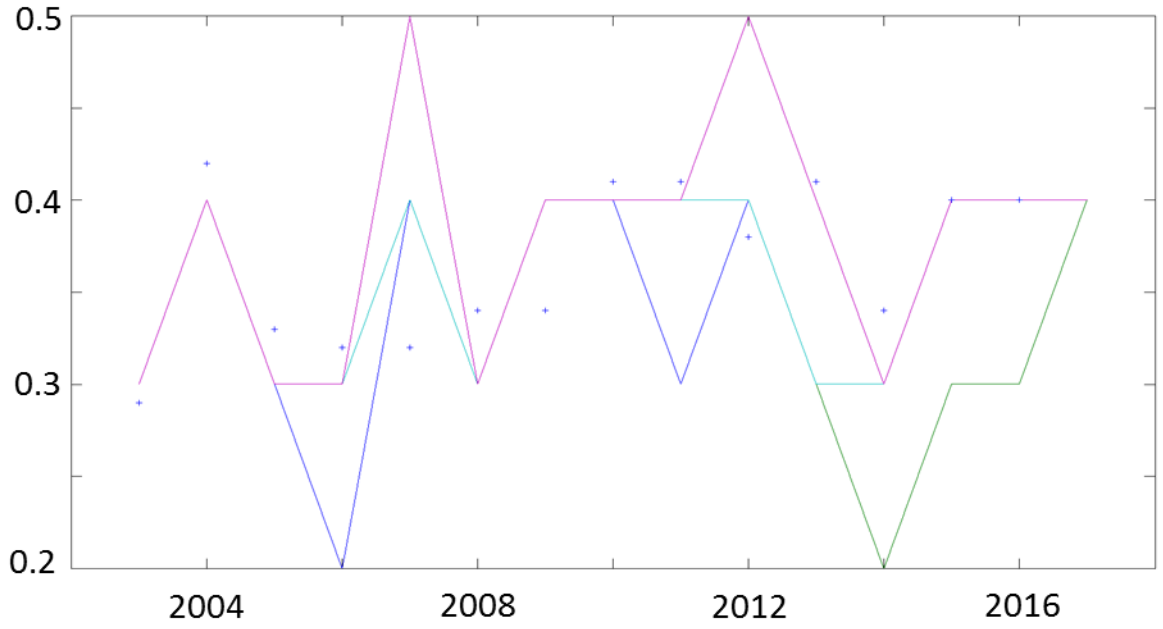

Fig 3: Modeled (lines) and measured (points) active layer thickness (unit m) at Barrow, Alaska, using an ensemble with five members, for the years 2003-2017.

Fig. 4: Modeled (lines) and measured (points) active layer thickness (unit m) at Nadym, Russia, using an ensemble with five members, for the years 2003-2017.

The two next figures (Fig. 5-6, Longyearbyen and Zackenberg) represent cases in which the CCI+ Permafrost scheme does not manage to represent measured active layer thickness too well. Both sites represent rather dry tundra sites, which are different from the relatively wet and organic-rich generic tundra stratigraphy assumed in the CCI+ Permafrost scheme.

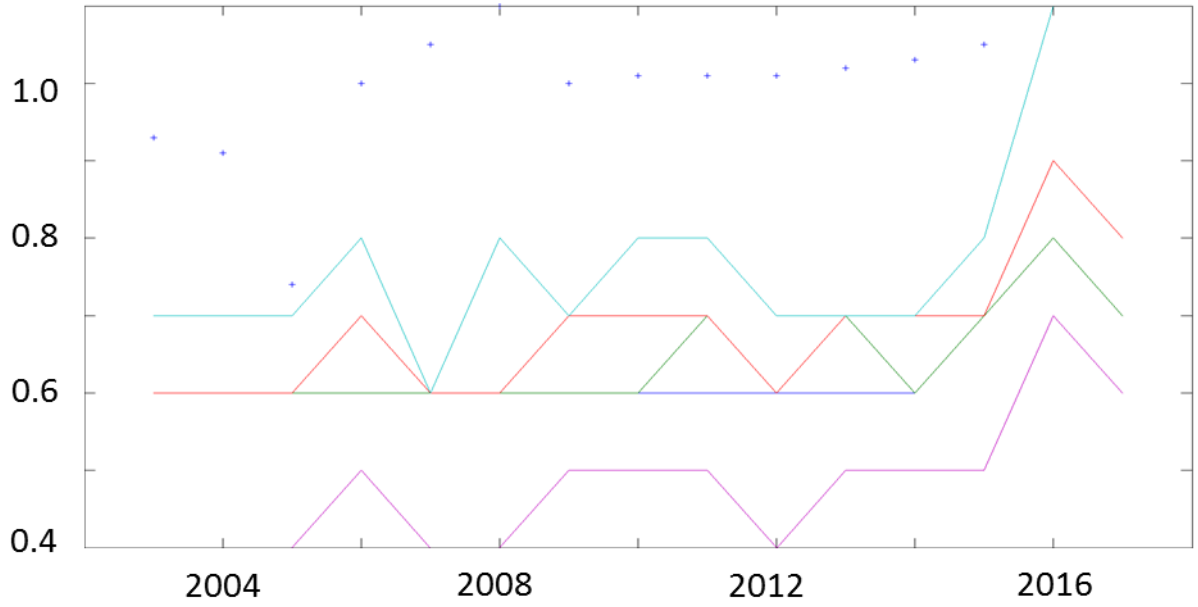

Fig. 5: Modeled (lines) and measured (points) active layer thickness (unit m) near Longyearbyen, Svalbard, using an ensemble with five members, for the years 2003-2017.

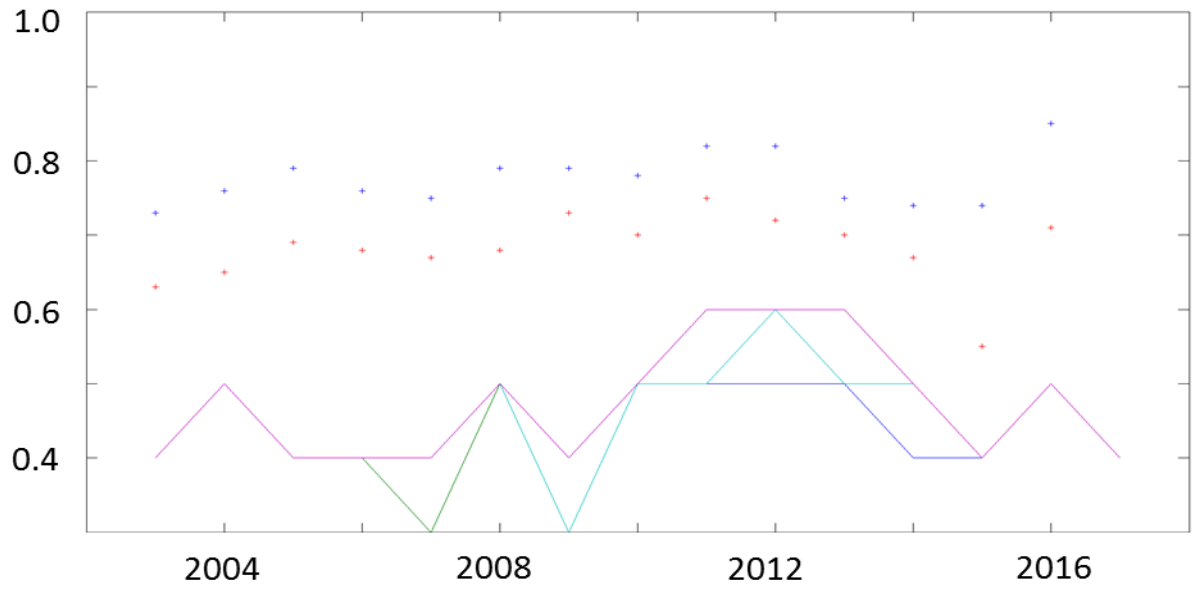

Fig 6: Modeled (lines) and measured (blue points: ZeroCALM 1, red points: ZeroCALM 2) active layer thickness (unit m) at Zackenberg, Greenland, using an ensemble with five members, for the years 2003-2017.

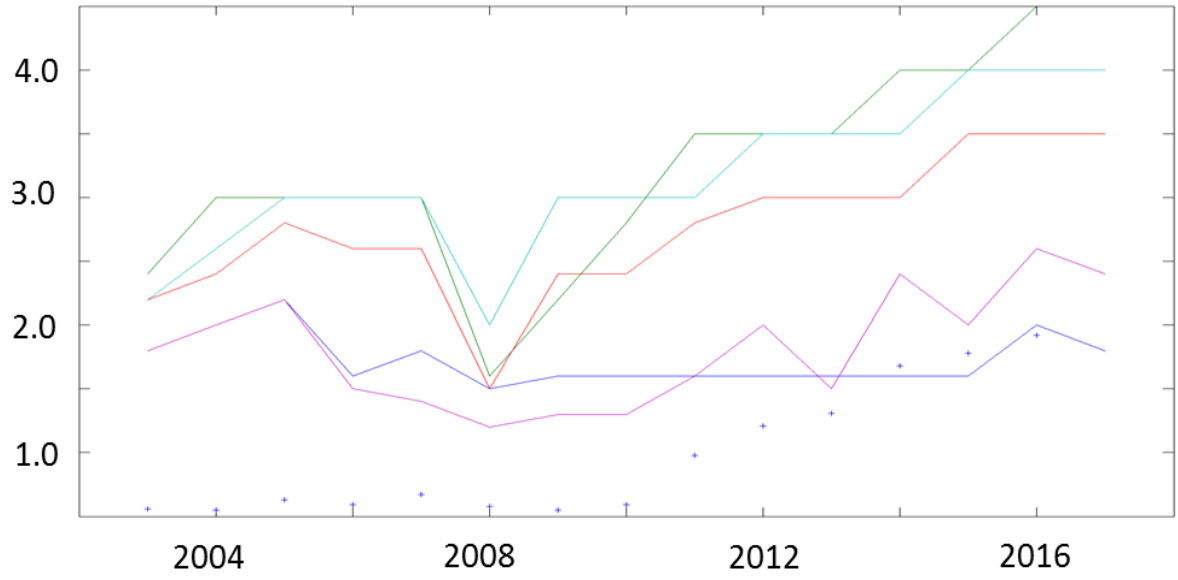

Fig. 7: Modeled (lines) and measured (points) active layer thickness (unit m) at Bonanza Creek, Alaska, using an ensemble with five members, for the years 2003-2017. The site burned in 2010, leading to destruction of the upper organic layer and a subsequent strong increase in active layer thickness.

The last figure (Fig. 7, Bonanza Creek) represents an interesting case in which the ground stratigraphy and surface properties changed strongly after a forest fire in 2011. While the CCI+ Permafrost algorithm considerably overestimates measured active layer thickness prior to the burn, the match is much improved with two of the ensemble members (corresponding to the tundra landcover class) after the burn. This once again shows that the strong effect of the ground stratigraphy on active layer thickness.

In summary, the CCI+ permafrost algorithm appears capable of reproducing measured active layer thickness at CALM sites, if suitable ground stratigraphies can be made available. This is an important point, since ground stratigraphy products are likely improved in the future, so that the performance regarding active layer thickness will gradually improve. Published global studies with global focus have reached an RMSE with respect to in-situ measurements of 0.53m (Aalto et al., 2018, using machine learning without EO data) and a correllation coefficient (R^2) of 0.7 (based on 303 individual sites), or a correlation coefficient of 0.76 (Park et al., 2016; no comparable RMSE provided). The user requirements outlined

Permafrost fraction: Only sparse in-situ evaluations of permafrost fraction are available, strongly complicating validation for this parameter (see Chadburn et al, 2017). A significant advantage of the Permafrost_cci algorithm (9) compared to all other algorithms, except (7), is that also ground surface temperatures can be employed for validation, not only temperatures measured in deeper layers. This makes it possible to directly employ temperature distributions provided by spatially distributed temperature logger arrays, which have been installed at several locations in the past five years. An example is presented in Fig. 8, showing the ensemble representation of the site in CryoGrid CCI. In this case, we conclude that the model ensemble is generally in the right temperature range, it is cold-biased by about 1 ºC (highest density of the ensemble members around -3 ºC instead of -2 ºC) and does not represent the "warmer" locations" between -1.5 and 0 ºC. Despite the small bias, the comparison clearly shows the strengths of the ensemble approach taken in Permafrost_cci, in that the scheme indeed represents a range of temperatures within a pixel instead of a single temperature as e.g. in methods (3) and (8).

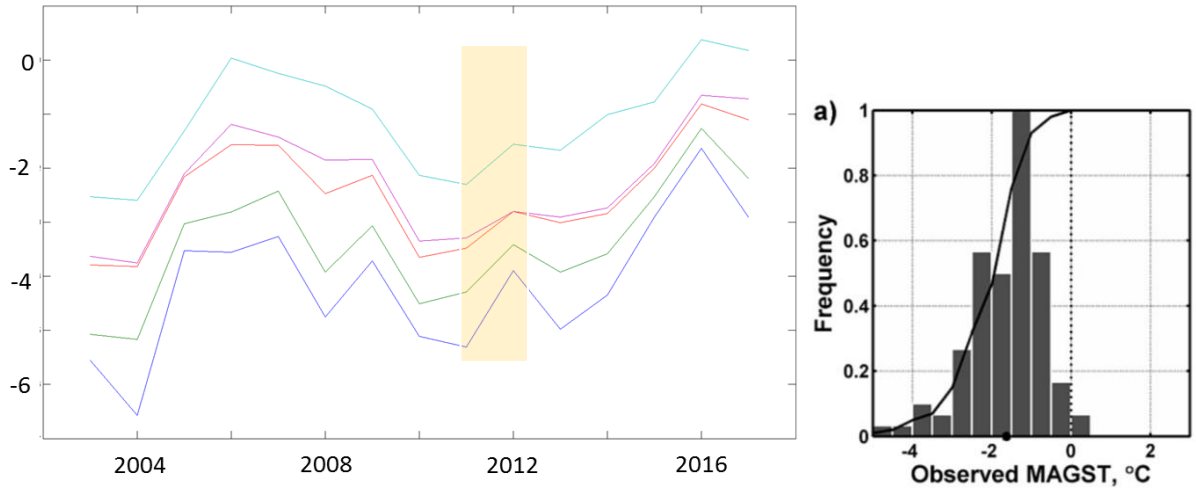

Fig. 8: Left: modeled annual average temperatures at the ground surface for the 1km pixel around the Bayelva permafrost observatory, Svalbard, using an ensemble with five members. The time period (2011/12) and range (ca. -5 to 0 ºC) of measured ground surface temperatures (right figure) are marked in light yellow. Right: Histogram of measured average ground surface temperatures 2011/12 based on 100 loggers within a 500 x 500m area within the pixel shown in the left (from Fig. 2 in Gisnås et al., 2014).

On larger scales, the modeling an ensemble instead of a single realization per pixel facilitates reproducing permafrost fractions and thus a gradual transition between permafrost and permafrost free locations (Obu et al., in review). In particular in mountain regions, where permafrost occurs highly localized and normally requires modelling at resolutions of at least tens of meters, the approach can play out its strength. Fig. 9 shows modelled permafrost fractions in the European Alps around. St. Moritz, Switzerland, compared to results of a high-resolution model run (compiled by Dr. Joel Fiddes, SLF Davos, Switzerland, as contribution to the Permafrost_cci round robin. His results represent a deterministic representation at effective pixel sizes of about 10m, taking the small-scale spatial variability of several factors into account. It generally shows that permafrost is restructured to the high elevations of the mountains, especially in northerly expositions. The 1km Permafrost_cci algorithm cannot deliver the same spatial detail, but clearly shows high permafrost fractions (yellow colour, right map), where large coherent areas of permafrost exist in the high-resolution map (left map). Furthermore, areas with only sparse and localized permafrost occurrences, such as in the area east (right) of St. Moritz, show up as low permafrost percentages (light blue colour) within 1km pixels, representing the sparse permafrost occurrence statistically. This suggests that the Permafrost_cci algorithm can deliver useful results even in highly structured areas, such as in the European Alps.

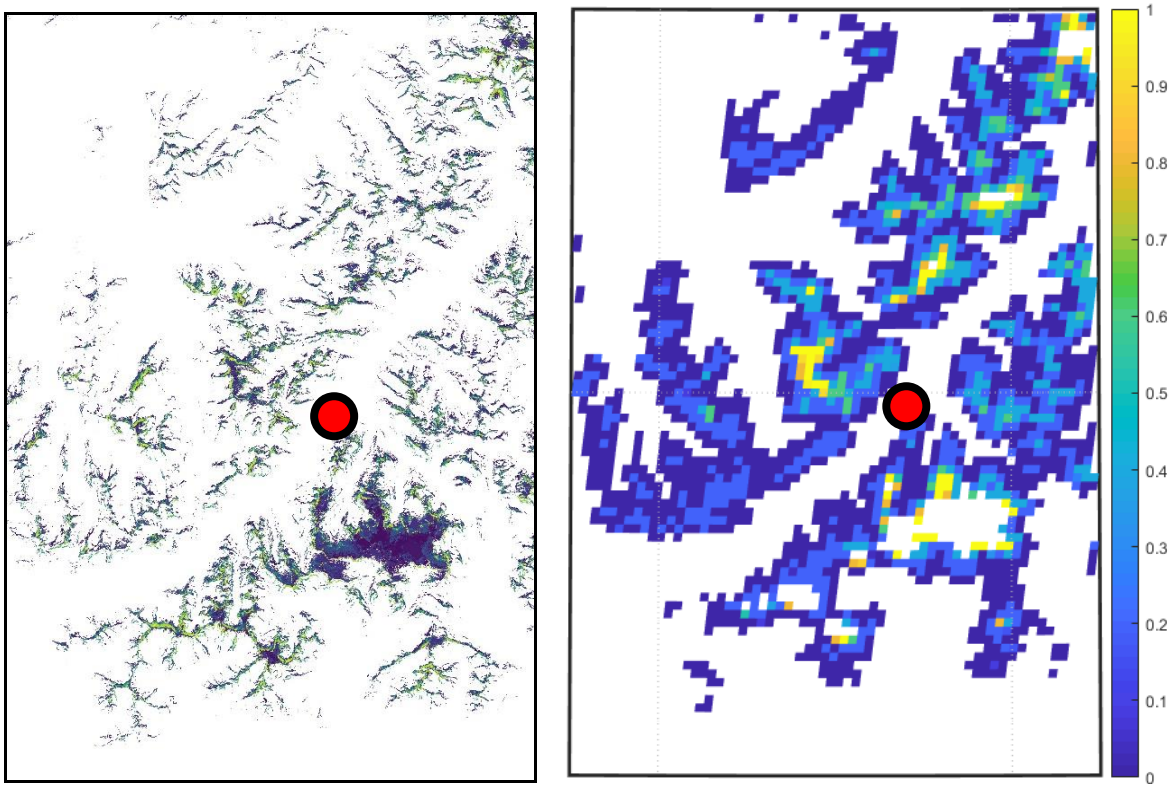

Fig. 9: Comparison of permafrost extent (right panel, probability coded as colours from 0 to 1) computed with the Permafrost_cci algorithm with high-resolution (10m) simulations compiled with the TopoScale-TopoSub-GeoTop2.0 scheme (Fiddes et al., 2015) for the area around St. Moritz (marked as red dot) in the European Alps. The simulations were provided by Joel Fiddes (SLF Davos, Switzerland), showing warm permafrost in dark blue and warm permafrost in yellow. The large spot south of St. Moritz (left map) is actually a glacier, so it has not been modeled with CryoGrid CCI (right map). The modeled area is approximately 20 x 40 km.

5 DISCUSSION AND ALGORITHM SELECTION

5.1 User needs

Permafrost_cci aims to provide global observations of permafrost that can addresses GCOS Action 33 in a consistent and comparable way [AD-1,3,4]. The Permafrost_cci algorithm based on the CryoGrid CCI driven by remotely sensed LST, snow cover information and the ESA CCI landcover product can deliver the two state variables of the permafrost ECV, ground temperature (K) and active layer thickness. Permafrost fraction, which is of interest for almost half of users who participated in the GlobPermafrost open user survey [RD-4,6], is delivered in addition. This also addresses the needs expressed by the IPA Action Group 'Specification of a Permafrost Reference Product in Succession of the IPA Map' [RD-5].

Table 3: Threshold (minimum) and target (optimal) requirements identified in the User Requirements Document (URD [RD-1], corresponding to Tables 1/2), and assessment of the likely performance of the Permafrost_cci Algorithm in year 1 and years 2/3. See text for details.

	Likely reached in year 1 (and years 2/3)
	Possibly reached in years 2/3
	Likely reached in years 2/3

	worse than threshold	**threshold**	**Between threshold and target**	**target**	**better than target**
Geographical coverage		Pan-Arctic		Global	
Temporal sampling		yearly		monthly	
Temporal extent		Last decade		1979 - present	
Horizontal resolution		10 km		1km	
Subgrid variability		no		yes	
Ground Temperature					
Vertical resolution		50 cm exponential		5 cm exponential	
Vertical extent		15 m		30 m	
Precision		0.5 K		0.1 K	
Accuracy		RMSE < 2.5°C		RMSE < 0.5°C	
Active Layer Thickness					
Precision		10 cm		1 cm	
Accuracy		RMSE < 25 cm		RMSE < 10 cm	

Following the assessment of the algorithm presented in Section 4, we establish a first assessment of the likely performance of the Permafrost_cci algorithm with respect to the User requirements. As summarized in Table 3, the threshold requirements of most parameters are expected to be reached in the year 1 of Permafrost_cci, with target requirements possibly or likely reached in the later stages of the project. In agreement with previous studies, active layer thickness is expected to be the most challenging variable, with the performance strongly dependent on the availability of a good ground stratigraphy product. Still, it is well possible to achieve threshold requirements with the CCI+ Permafrost algorithm, judging from the good performance for some of the investigated sites (Figs. 3 and 4). The target requirements for both ground temperature (0.5 K) and active layer thickness (0.1m) are considerably smaller than the spatial variability of these parameters within 1km pixels, so that it seems impossible to reach these values when comparing 1km statistics to in-situ measurements taken for points or at least much smaller areas.

Following the presentation of a first EO-based permafrost map in the ESA GlobPermafrost project (Obu et al., in review), the Permafrost_cci algorithm can add transient changes of permafrost which are important to assess the effects of climate change on permafrost. For the climate modeling community, the new products are likely to be much improved compared to GlobPermafrost, since depth- and time-specific information on the permafrost ECV can be provided, which can be directly compared to the output of Earth System Models.

5.2 Algorithm consistency and suitability for change detection

The Permafrost_cci algorithm is based on a transient permafrost model that delivers both active layer thickness and ground temperature from driving data based on EO-products. This makes the results inherently consistent between the two physical state variables. Consistency in time is also guaranteed, at least if the input driving data are consistent in time. Here, Permafrost_cci will use the data from other CCI+ projects as much as possible, especially LST_cci and Snow_cci, in which consistency over time is a major goal. The Permafrost_cci algorithm is highly suited for change detection, since the thermal inertia of the ground and the effect of different ground stratigraphies are explicitly taken into account. Except for a few caveats for active layer thickness (fires and excess ice melt, see Sect. 4.3), a consistent performance with respect to change detection can be expected. The Permafrost_cci algorithm in particular facilitates detection of talik formation, which is highly important to detect and quantify the impacts of climate change on permafrost.

5.3 Technical consideration

The main challenge of the transient Permafrost_cci algorithm is the considerable computational costs. Taking “1 model year and grid cell/model realization” as a base unit, running the CryoGrid CCI model for the entire global permafrost domain in ensemble model (method 9) is between factor of 100 to factor 1000 larger than what has been accomplished in previous studies with transient permafrost

models (e.g. Jafarov et al., 2012; Wang et al., 2018), which demonstrates the considerable difficulty of the task. For this reason, the algorithm has been strongly improved with respect to runtime (see Sect. 4.1), and implemented in a scalable fashion on the Abel Supercomputing cluster at the University of Oslo. All parts of the processing chain have by now been tested for scalability, and the results indicate that it is feasible to model the entire permafrost domain (ca. 25 Mio km^2) for the period 2003-2017 with five ensemble members per grid cell which allows assigning the zones continuous (all ensemble members permafrost), discontinuous (3-4 ensemble members permafrost) and sporadic (1-2 ensemble members permafrost) permafrost. The runtime of "1 model year and ensemble member" is about 0.1sec, suggesting a computational requirement of less than 100,000 CPU hours for the entire processing, which we have confirmed for year 1 of Permafrost_cci (project number N9606 on the Abel cluster). We conclude that CCI+ algorithm is readily implemented and its scalability tested, suggesting that it is feasible to produce the Permafrost_cci products at the specifications outlined in Sect. 5.1.

6 BIBLIOGRAPHY AND ACRONYMS

6.1 Bibliography

Aalto, J., Karjalainen, O., Hjort, J. and Luoto, M., 2018. Statistical forecasting of current and future circum-Arctic ground temperatures and active layer thickness. Geophysical Research Letters, 45(10), 4889-4898.

Brown R.J.E., 1970: Permafrost in Canada: Its influence on northern development. University of Toronto Press, Toronto 234 p.

Brown, J., Ferrians Jr, O. J., Heginbottom, J. A., & Melnikov, E. S. (1997). Circum-Arctic map of permafrost and ground-ice conditions (p. 45). Reston: US Geological Survey.

Biskaborn, B. K., Lanckman, J. P., Lantuit, H., Elger, K., Dmitry, S., William, C., & Vladimir, R. (2015). The new database of the Global Terrestrial Network for Permafrost (GTN-P). Earth System Science Data, 7, 245-259.

Chadburn, S. E., Burke, E. J., Cox, P. M., Friedlingstein, P., Hugelius, G., & Westermann, S. (2017). An observation-based constraint on permafrost loss as a function of global warming. Nature Climate Change, 7(5), 340.

Daanen, R. P., Ingeman-Nielsen, T., Marchenko, S. S., Romanovsky, V. E., Foged, N., Stendel, M., ... & Hornbech Svendsen, K. (2011). Permafrost degradation risk zone assessment using simulation models. The Cryosphere, 5(4), 1043-1056.

Fiddes, J., Endrizzi, S., & Gruber, S. (2015). Large-area land surface simulations in heterogeneous terrain driven by global data sets: application to mountain permafrost. The Cryosphere, 9(1), 411-426.

Gangodagamage, C., Rowland, J. C., Hubbard, S. S., Brumby, S. P., Liljedahl, A. K., Wainwright, H., Wilson, C. J., Altmann, G. L., Dafflon, B., Peterson, J., Ulrich, C., Tweedie, C. E., and Wullschleger, S. D.: Extrapolating active layer thickness measurements across Arctic polygonal terrain using Li-DAR and NDVI data sets, Water Resour. Res., 50, 6339–6357, doi:10.1002/2013WR014283, 2014.

Gisnås, K., Westermann, S., Schuler, T. V., Litherland, T., Isaksen, K., Boike, J., & Etzelmüller, B. (2014). A statistical approach to represent small-scale variability of permafrost temperatures due to snow cover. The Cryosphere, 8, 2063-2074.

Heginbottom, J.A., 1984: The mapping of permafrost. Canadian Geographer, Vol. 28, No.1, pp. 78-83.

Heginbottom, J.A., Radburn, L.K., 1992: Permafrost and Ground Ice Conditions of Northwestern Canada (Mackenzie Region). National Snow and Ice Data Center, Boulder, CO, USA.

International Permafrost Association (2010). https://gtnp.arcticportal.org/

Jafarov, E. E., Marchenko, S. S., & Romanovsky, V. E. (2012). Numerical modeling of permafrost dynamics in Alaska using a high spatial resolution dataset. The Cryosphere, 6(3), 613-624.

Kelley, A. M., Epstein, H. E., and Walker, D. A.: Role of vegetation and climate in permafrost active layer depth in arctic tundra of northern Alaska and Canada, J. Glaciol. Climatol., 26, 269–273, 2004.

Kroisleitner, C., Bartsch, A., & Bergstedt, H. (2018). Circumpolar patterns of potential mean annual ground temperature based on surface state obtained from microwave satellite data. Cryosphere, 12(7).

Kudryavtesv V.A., (Editor) 1978: Obshcheye merzlotovedeniya (Geokriologiya) (General permafrost science) In Russian. Izd. 2, (Edu 2) Moskva (Moscow), Izdatel'stvo Moskovskogo Universiteta, (Moscow University Editions), 404 p

Langer, M., Westermann, S., Heikenfeld, M., Dorn, W., & Boike, J. (2013). Satellite-based modeling of permafrost temperatures in a tundra lowland landscape. Remote Sensing of Environment, 135, 12-24.

Leverington, D. W. and Duguay, C. R.: Evaluation of Three Supervised Classifiers in Mapping “Depth to Late-Summer Frozen Ground”, Central Yukon Territory, Can. J. Remote Sens., 22, 2, doi:10.1080/07038992.1996.10874650, 1996.

Liu, L., Zhang, T., & Wahr, J. (2010). InSAR measurements of surface deformation over permafrost on the North Slope of Alaska. Journal of Geophysical Research: Earth Surface, 115(F3).

Liu, L., Schaefer, K., Zhang, T., & Wahr, J. (2012). Estimating 1992–2000 average active layer thickness on the Alaskan North Slope from remotely sensed surface subsidence. Journal of Geophysical Research: Earth Surface, 117(F1).

McMichael, C. E., Hope, A. S., Stow, D. A., and Fleming, J. B.: The relation between active layer depth and a spectral vegetation index in arctic tundra landscapes of the North Slope of Alaska, Int. J. Remote Sens., 18, 11, doi:10.1080/014311697217666, 1997.

Muller S.W, 1943: Permafrost or permanently frozen ground and related engineering problems. U.S. Engineers Office, Strategic Engineering Study, Special Report No. 62. 136p. (Reprinted in 1947, J. W. Edwards, Ann Arbor, Michigan, 231p.)

Nelson, F. E., Shiklomanov, N. I., Mueller, G. R., Hinkel, K. M., Walker, D. A., and Bockheim, J. G.: Estimating Active-Layer Thickness over a Large Region: Kuparuk River Basin, Alaska, USA, Arctic Alpine Res., 29, 4, doi:10.2307/1551985, 1997.

Nitze, I., & Grosse, G. (2016). Detection of landscape dynamics in the Arctic Lena Delta with temporally dense Landsat time-series stacks. Remote Sensing of Environment, 181, 27-41.

Obu, J., Westermann, S., Bartsch, A., Berdnikov, N., Christiansen, H., Dashtseren, D., Delaloye, R., Elberling, B., Etzelmüller, B., Kholodovh, A., Khomutov, A., Kääb, A., Leibman, M., Lewkowicz, A., Panda, S., Romanovsky, V., Way, R., Westergaard-Nielsen, A., Wu, T., Yamkin, J., & Zou, D.: Northern Hemisphere permafrost map 2000-2016 based on TTOP modelling at 1 km scale, Earth-Science Reviews, in review.

Park, H., Kim, Y., & Kimball, J. S. (2016). Widespread permafrost vulnerability and soil active layer increases over the high northern latitudes inferred from satellite remote sensing and process model assessments. Remote Sensing of Environment, 175, 349-358.

Peddle, D. R. and Franklin, S. E.: Classification of permafrost active layer depth from remotely sensed and topographic evidence, Remote Sens. Environ., 44, 1, doi:10.1016/0034-4257(93)90103-5, 1993.

Schaefer, K., Liu, L., Parsekian, A., Jafarov, E., Chen, A., Zhang, T., ... & Schaefer, T. (2015). Remotely sensed active layer thickness (ReSALT) at Barrow, Alaska using interferometric synthetic aperture radar. Remote Sensing, 7(4), 3735-3759.

Sorg, A., Kääb, A., Roesch, A., Bigler, C., & Stoffel, M. (2015). Contrasting responses of Central Asian rock glaciers to global warming. Scientific Reports, 5, 8228.

Strozzi, T., Antonova, S., Günther, F., Mätzler, E., Vieira, G., Wegmüller, U., ... & Bartsch, A. (2018). Sentinel-1 SAR Interferometry for Surface Deformation Monitoring in Low-Land Permafrost Areas. Remote Sensing, 10(9), 1360.

Westermann, S., Schuler, T., Gisnås, K., & Etzelmuller, B. (2013). Transient thermal modeling of permafrost conditions in Southern Norway. The Cryosphere, 7(2), 719-739.

Westermann, S., Elberling, B., Højlund Pedersen, S., Stendel, M., Hansen, B. U., & Liston, G. E. (2015). Future permafrost conditions along environmental gradients in Zackenberg, Greenland. The Cryosphere, 9(2), 719-735.

Westermann, S., Langer, M., Boike, J., Heikenfeld, M., Peter, M., Etzelmüller, B., & Krinner, G. (2016). Simulating the thermal regime and thaw processes of ice-rich permafrost ground with the land-surface model CryoGrid 3. Geoscientific Model Development Discussions, 9, 523-546.

Westermann, S., Peter, M., Langer, M., Schwamborn, G., Schirrmeister, L., Etzelmüller, B., & Boike, J. (2017). Transient modeling of the ground thermal conditions using satellite data in the Lena River delta, Siberia. The Cryosphere, 11(3), 1441.

Widhalm, B., A.Bartsch, M.B.Siewert, G.Hugelius, B.Elberling, M.Leibman, Y.Dvornikov, and A.Khomutov (2016): Site scale wetness classification of tundra regions with C-band SAR satellite data, in Proc. 'Living Planet Symposium 2016', Prague, Czech Republic, ESA SP-740.

Widhalm, B., Bartsch, A., Leibman, M., and Khomutov, A. (2017): Active-layer thickness estimation from X-band SAR backscatter intensity, The Cryosphere, 11, 483-496, https://doi.org/10.5194/tc-11-483-2017.

Williams, J.R., 1965: Ground water in permafrost regions: An annotated bibliography. U.S. Geological Survey, Professional Paper 696, 83p.

van Everdingen R.O., 1985: Unfrozen permafrost and other taliks. Workshop on Permafrost Geophysics, Golden, Colorado, October 1984 (J. Brown, M.C. Metz, P. Hoekstra, Editors). U.S. Army, C.R.R.E.L., Hanover, New Hampshire, Special Report 85-5, pp.101-105

Wang, K., Overeem, I., Zhang, T., Jafarov, E.: High Spatial Resolution Soil Temperatures Simulation over the Northern Hemisphere, Poster C33F-163, AGU Fall Meeting 2019, Washington USA.

6.2 Acronyms

AD	Applicable Document
ALT	Active Layer Thickness
AWI	Alfred Wegener Institute Helmholtz Centre for Polar and Marine Research
B.GEOS	b.geos GmbH
CALM	Circumpoler active layer monitoring network
CCI	Climate Change Initiative
CMUG	Climate Modelling User Group
CRG	Climate Research Group
CRS	Coordinate Reference System
DARD	Data Access Requirements Document
ECV	Essential Climate Variable
EO	Earth Observation
ESA	European Space Agency
ESA DUE	ESA Data User Element
GAMMA	Gamma Remote Sensing AG
GCOS	Global Climate Observing System
GCMD	Global Change Master Directory
GIPL	Geophysical Institute Permafrost Laboratory
GTD	Ground Temperature at certain depth
GTN-P	Global Terrestrial Network for Permafrost
GUIO	Department of Geosciences University of Oslo
IPA	International Permafrost Association
IPCC	Intergovernmental Panel on Climate Change
LST	Land Surface Temperature
MAGT	Mean Annual Ground Temperature
MAGST	Mean Annual Ground Surface Temperature
NetCDF	Network Common Data Format

NSIDC	National Snow and Ice Data Center
PFR	Permafrost extent (Fraction)
PFF	Permafrost-Free Fraction
PFT	Permafrost underlain by Talik
PSD	Product Specifications Document
PSTG	Polar Space Task Group
PZO	Permafrost Zone
RD	Reference Document
RMSE	Root Mean Square Error
RS	Remote Sensing
SLF	Institut für Schnee- und Lawinenforschung, Davos
SU	Department of Physical Geography Stockholm University
TSP	Thermal State of Permafrost
UAF	University of Alaska, Fairbanks
UNIFR	Department of Geosciences University of Fribourg
URD	Users Requirement Document
WGS 84	World Geodetic System 1984